

# Conformational Analysis of Aliskiren, a Potent Renin Inhibitor, Using High-Resolution Nuclear Magnetic Resonance and Molecular Dynamics Simulations

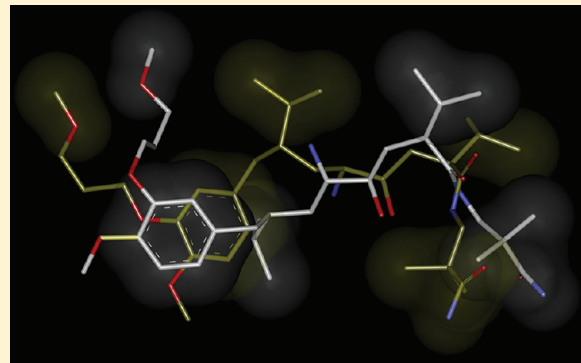
Minos-Timotheos Matsoukas,<sup>†</sup> Panagiotis Zoumpoulakis,<sup>‡</sup> and Theodore Tselios<sup>\*†</sup>

<sup>†</sup>Department of Chemistry, University of Patras, GR-26504, Rion, Patras, Greece

<sup>‡</sup>Laboratory of Molecular Analysis, Institute of Organic and Pharmaceutical Chemistry, National Hellenic Research Foundation, 48 Vas. Constantinou Avenue, GR-11635 Athens, Greece

 Supporting Information

**ABSTRACT:** Aliskiren is a nonpeptide antihypertensive drug that potently inhibits the human enzyme renin in vitro and in vivo. Many clinical trials have shown the efficacy of aliskiren to lower blood pressure in correlation with other antihypertensive agents. In this report, the conformational behavior of aliskiren is studied in water, trifluoroethanol, and dimethylformamide solutions by means of 2D-NMR spectroscopy and molecular dynamics simulations. The stereochemical characteristics of aliskiren in different solutions, in combination with the previously published crystal structure of the renin–aliskiren complex have been investigated. The aim of this study was to explore the conformational behavior of this first successful renin inhibitor in relation to its environment. In aqueous solution, aliskiren adapts a U-shape conformation, whereas in DMF, the molecule is basically endowed with an “extended” conformation, which has more similarities to the one bound to the receptor.



## ■ INTRODUCTION

The Renin–Angiotensin–Aldosterone System (RAAS) has a central role in the regulation of blood pressure as well as in the maintenance of sodium and electrolyte balance. A sequence of enzyme reactions leads to the release of Angiotensin II (Ang II), a potent vasoconstrictive hormone.<sup>1</sup> The biosynthesis of this peptide starts from an enzyme reaction between renin, a highly selective aspartic protease and angiotensinogen, which leads to a decapeptide, Angiotensin I (Ang I). Thereinafter, Ang I is cleaved in position 8 by the angiotensin-converting enzyme (ACE) to produce the octapeptide hormone Ang II. It is known that Ang II is as well produced by other biological pathways besides ACE and Ang I. These pathways invoke enzymes such as the chymostatin-sensitive Ang II-generating enzyme, chymase, human cardiac chymase, cathepsin G, the tissue plasminogen activator, cathepsin G, and tonin.<sup>2</sup> Most effects produced by Ang II are the result of its binding to Angiotensin II type 1 receptors<sup>3</sup> (AT<sub>1</sub>R) leading to vasoconstriction. Moreover, AT<sub>1</sub>R activation results to aldosterone release, which enhances Na<sup>+</sup> and K<sup>+</sup> excretion. Intervention of this cascade has been investigated as a treatment option for hypertension and congestive heart failure.<sup>4</sup> Because the formation of Ang II is accomplished through two enzymatic events mediated by renin (functioned at the first rate-limiting step) and an angiotensin-converting enzyme (ACE), it is thus believed that inhibition of renin or ACE results in antihypertensive effects. Furthermore, given the fact that angiotensinogen is the

only known naturally occurring substrate for renin (in contrast to the multiple substrates known for ACE), this has rendered renin as an ideal target for the development of antihypertensive drugs.<sup>5</sup>

Many potential drug agents targeting renin have been developed by the pharmaceutical industry, including enalkiren, remikiren, and zankiren,<sup>6,7</sup> but without success. The development of other agents of this class is highly anticipated as a few are pending.<sup>8</sup> The only orally active renin inhibitor that is available in the market, aliskiren,<sup>9–12</sup> has been successfully tested for preclinical and clinical evaluation.<sup>13</sup> The innovativeness of aliskiren, the first in a novel class of orally active, nonpeptide, highly specific, human renin inhibitors, has given a great boost to the research field of renin enzyme and its effect on the Renin–Angiotensin–Aldosterone System (RAAS). This has resulted in several studies regarding the newly introduced drug aliskiren to the pharmaceutical industry as an antihypertensive drug with various effects, specifically the blockade of the Renin receptor. Renin inhibitors constitute a new generation of nonpeptidic drugs for the treatment of hypertension with the attenuation of side effects<sup>14–16</sup> either administered alone or combined with other RAAS modulators.<sup>17,18</sup>

Received: March 18, 2011

Published: July 21, 2011

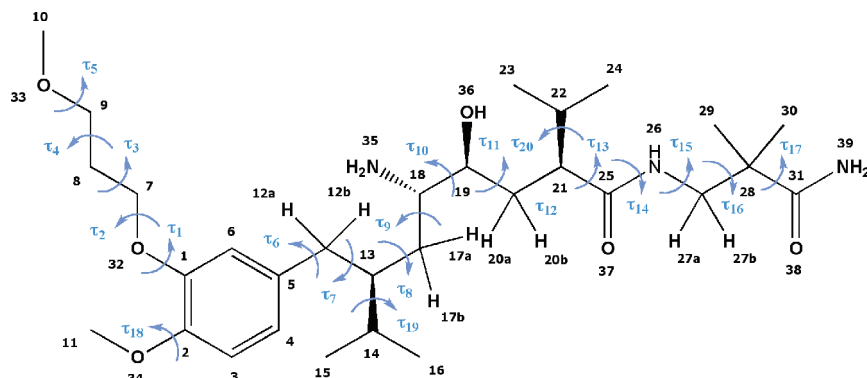


**Figure 1.** Chemical structure of aliskiren,  $C_{30}H_{53}N_3O_6$ . Numbering for NMR assignment is according to Waldmeier et al.,<sup>24</sup> and dihedral angles  $\tau_1-\tau_{20}$  are indicated on the structure.

**Table 1.** NMR Chemical Shifts of aliskiren in  $D_2O$ ,  $DMF-d_7$ ,  $TFE-d_3$ , and  $TFE-d_3/D_2O$  Solutions

$n$	chemical shifts ( $\delta$ /ppm)							
	$\Delta\nu^1H D_2O -$		$\Delta\nu^1H D_2O -$		$\Delta\nu^1H D_2O -$		$\Delta\nu^{13}C D_2O$	
	$^1H D_2O$	$^1H DMF-d_7$	$^1H DMF-d_7$ (ppm)	$^1H TFE-d_3/D_2O$	$^1H TFE-d_3/D_2O$ (ppm)	$^1H TFE-d_3$	$^1H TFE-d_3$ (ppm)	
1								146.93
2								146.35
3	6.86	6.89	0.03	7.15	0.29	6.85	-0.01	111.86
4	6.74	6.78	0.04	7.23	0.49	6.93	0.19	121.59
6	6.78	6.91	0.13	7.06	0.28	6.75	-0.03	113.90
7	3.98	4.03	0.05	4.34	0.36	3.98	0.00	65.49
8	1.91	1.97	0.06	2.30	0.39	1.91	0.00	27.96
9	3.49	3.49	0.00					66.65
10	3.22	3.27	0.05	3.62	0.40	3.31	0.09	55.30
11	3.69	3.78	0.09	4.06	0.37	3.75	0.06	57.42
12a	2.57	2.63	0.06	2.58	0.01	2.27	-0.30	36.00
12b	2.25	2.49	0.24					
13	1.58	2.02	0.44	2.34	0.76	2.02	0.44	41.52
14	1.56	1.67	0.11	2.00	0.44	1.69	0.13	29.46
15	0.79	0.84	0.05	1.23	0.44	0.92	0.13	19.62
16	0.75	0.86	0.11	1.14	0.39	0.84	0.09	19.99
17a	1.38	1.69	0.31	1.91	0.53	1.61	0.23	30.48
17b	1.35	1.54	0.19	2.02	0.67	1.71	0.36	
18	2.43	3.05	0.62					55.52
19	3.05			3.01	-0.04	2.71	-0.34	68.65
20a	1.10	1.83	0.73	1.68	0.58	1.37	0.27	32.62
20b	1.43	1.51	0.08	1.79	0.36	1.48	0.05	
21	2.05	2.40	0.35					49.41
22	1.52	1.78	0.26	2.06	0.54	1.75	0.23	30.48
23	0.74	0.90	0.16	1.17	0.43	0.86	0.12	17.42
24	0.73	0.88	0.15	1.16	0.43	0.85	0.12	17.34
27a	3.26	3.31	0.05	3.67	0.41	3.36	0.10	46.67
27b	3.14	3.38	0.24	3.52	0.38	3.22	0.08	
29	1.03	1.15	0.12	1.45	0.42	1.14	0.11	22.38
30	1.04	1.16	0.12	1.46	0.42	1.15	0.11	22.41

The de novo design and synthesis of peptide mimetics, which are stable to enzymatic degradation, is a central field of medicinal chemistry. NMR spectroscopy is well recognized as a powerful tool for the conformational study of biologically important compounds.<sup>19</sup> A combination of advanced 2D-NMR and molecular

modeling techniques<sup>20–22</sup> has proved to be the cornerstone in the rational drug design of potent nonpeptide mimetics.

Aliskiren (Figure 1) is a nonpeptidic renin inhibitor that specifically and potently inhibits human renin in vitro. In vivo, oral doses have shown blood pressure lowering in sodium-depleted

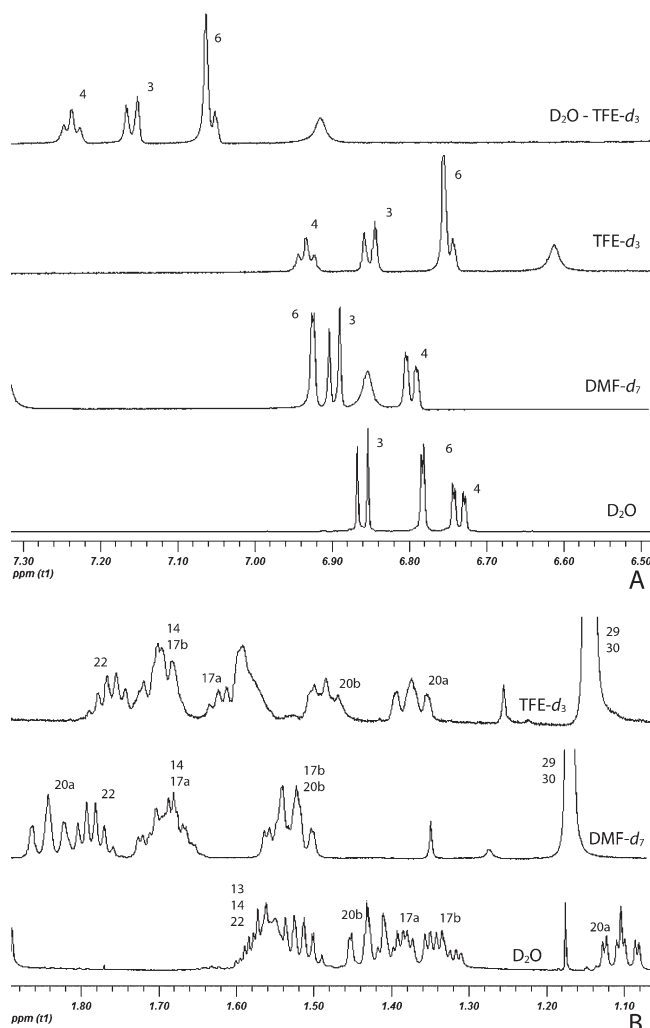


**Figure 2.** (a) Aromatic region (6.5–7.3 ppm) of the <sup>1</sup>H NMR spectrum of aliskiren in the four different solvent systems. (b) Differences in the 1.2–1.9 ppm region where a broadening effect is observed in the DMF-d<sub>7</sub> and TFE-d<sub>3</sub> spectra, as well as a spread in the chemical shifts.

marmosets, indicating its potency as an antihypertensive drug.<sup>23</sup> In previous studies, 1D-NMR experiments have been performed on aliskiren,<sup>24</sup> but no structural data is available in terms of its stereochemical characteristics in solution.

In the present study, we have applied high-resolution NMR spectroscopy in different solvents and compared the results in order to examine the structural characteristics of aliskiren. Data extracted on the interatomic distances between the functional groups of the molecule were combined with molecular modeling techniques for inspection and evaluation of the drug's molecular properties. These findings were used to compare the structure with the one cocrystallized with the human renin receptor<sup>25</sup> in order to provide information on the transformational changes and flexibility of the molecule and extract valuable data on the rational design of novel renin inhibitors. The NMR studies were performed in D<sub>2</sub>O, TFE-d<sub>3</sub>, and DMF-d<sub>7</sub> solutions in order to examine the conformational behavior, especially in D<sub>2</sub>O and DMF and to compare the obtained conformations in a polar (H<sub>2</sub>O, dielectric constant 81 at 25 °C) and an aprotic–lipophilic solvent (DMF, dielectric constant 37 at 25 °C). We show that the conformations obtained in these two environments have essential

differences, according to cross-peak values on the different solvents and also focus on differences compared to the bound form of the molecule to the renin receptor.

## ■ EXPERIMENTAL SECTION

**1. NMR Spectroscopy.** Aliskiren was purchased from Xing-cheng Chempharm Co., Ltd. (Taizhou, CH). NMR spectra were recorded on a Varian 600 MHz spectrometer. The sample concentration used in NMR studies was ca. 10 mM dissolved in D<sub>2</sub>O, DMF-d<sub>7</sub>, TFE-d<sub>3</sub>, and TFE-d<sub>3</sub>/D<sub>2</sub>O (1:1). Two dimensional homonuclear (COSY, ROESY) (SF1) and heteronuclear (HSQC, HMBC) (SF2,3) NMR techniques performed with gradients were used to structurally elucidate aliskiren in different environments. A 2D ROESY experiment was carried out using a mixing time of 250 ms, which ensures the operation at the initial linear part of the NOE buildup curve and the PRESAT sequence in order to suppress the water signal. The <sup>1</sup>H spectral width (SW) used was 6000 Hz.

The homonuclear 2D proton spectra were obtained with 4096 data points in t<sub>2</sub> dimension, 32 scans, 256–512 points in t<sub>1</sub> dimension, a relaxation delay of 1–1.5 s, and a SW of 30000 Hz. The <sup>1</sup>H–<sup>13</sup>C heteronuclear experiments were obtained with 1024–4096 data points in t<sub>2</sub> dimension and 32–64 scans and 256–512 points in t<sub>1</sub> dimension. Experimental data were processed using MestReNova software. Interatomic proton–proton distances were calculated using the two-spin approximation, and the integrated cross-peak intensity of a pair of adjacent aromatic protons was assumed to have a distance of 2.46 Å. The resulting distances were corrected for the frequency offset effects to be eliminated.<sup>26</sup> Upper and lower limit values of constraints were allowed (5% of toleration).

**2. Conformational Analysis.** All computer calculations were performed on a Pentium IV 2.14 GHz workstation using Discovery Studio version 2.0 molecular modeling systems by Accelrys Software, Inc. (San Diego, CA). The conformational space of aliskiren was explored using random sampling algorithms. The starting conformation was sketched in 2D and was subjected to an unrestrained conformational search on Discovery Studio with the Generate Conformations protocol and the BEST method, which includes random conformation search and torsion search algorithms and ensures the best coverage of conformational space. Aliskiren hemifumarate has four chiral centers, all were S configured. An implicit solvent model was applied, along with the SHAKE algorithm,<sup>27</sup> which was also implemented to satisfy bond geometry constraints and keep fixed bond lengths during all simulations. The dielectric constant ( $\epsilon$ ) was set to 58 as the mean value of H<sub>2</sub>O ( $\epsilon = 81$ ) and DMF ( $\epsilon = 37$ ) in order to simulate in the most approximate way the various mixtures of solvents used in the NMR studies.

Among the 1000 conformers extracted, the ones that satisfied the critical ROE interatomic distances were chosen. These were assigned as the starting conformers in order to apply the constraints on the molecular dynamics simulations.

**3. Molecular Dynamics.** MD runs were performed without torsional restraints, and all potential energy calculations were done according to the CHARMM force field. Two sets of dynamics protocols were implemented on the starting conformations: (a) distance restrained with a 5% tolerance of the provided restraints from the ROE experiments and (b) unrestrained dynamics as control runs. The procedure included an initial minimization stage for 200 steps, using the robust steepest

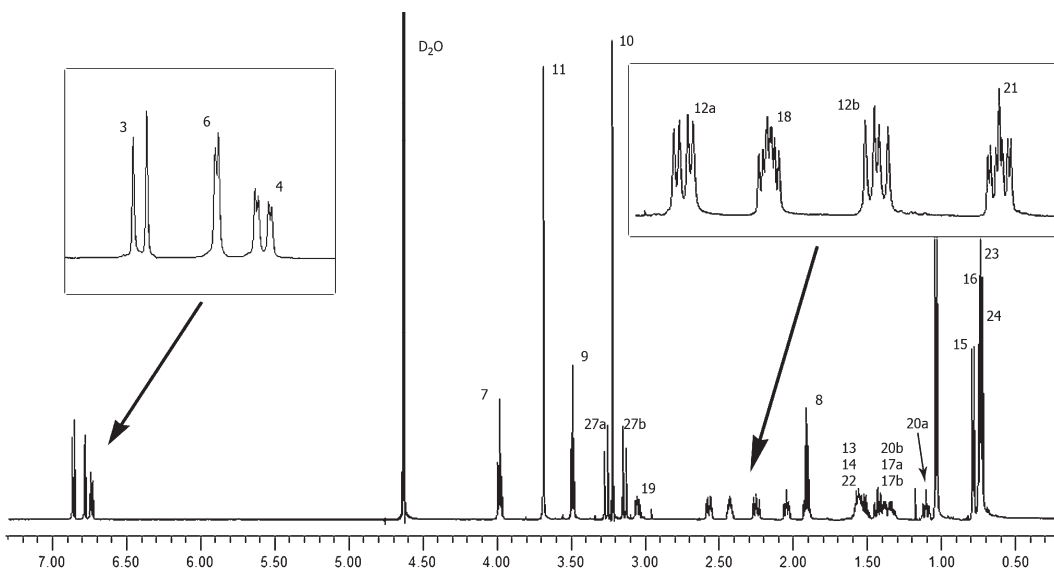


**Figure 3.**  $^1\text{H}$  NMR spectrum of aliskiren obtained at 25 °C in  $\text{D}_2\text{O}$  solvent. The 6.50–7.00 ppm and 2.00–2.70 ppm regions are magnified for better clarity of the reported peaks.

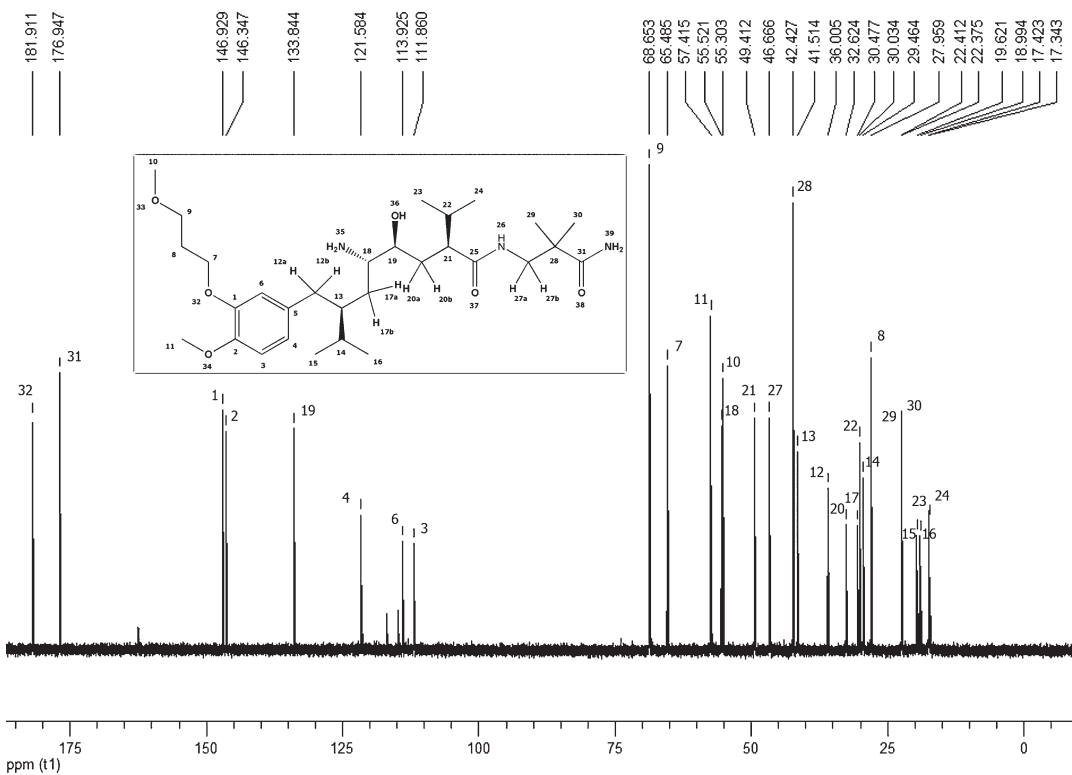


**Figure 4.**  $^{13}\text{C}$  NMR spectrum of aliskiren at 25 °C in  $\text{D}_2\text{O}$  along with the corresponding numbering of the molecule's carbons (top).

descent (SD) algorithm to resolve any initial poor contacts within the system without creating large distortions in the overall structure. A second minimization stage for 200 steps used the Adopted Basis Newton–Raphson (ABNR) method, where initial poor contacts are relieved to ensure that a low energy starting point is supplied to subsequent dynamics stages. Thereinafter, a heating stage was employed to add thermal energy to the system to reach a target temperature. The heating simulation was followed by an equilibration stage that ensures the energy in

the system is distributed appropriately among all degrees of freedom and allows the system to achieve thermal equilibration at the target temperature. Consecutively, a production stage was implemented that performs an employment of molecular dynamics in a controlled temperature statistical ensemble using a leapfrog Verlet integration algorithm from which structural and energetic properties are calculated. Finally, 300 minimization steps with the Conjugate Gradient algorithm (CG) were applied to relax the generated conformations and remove steric overlaps.

The above simulation temperatures were set for heating from 0 to 300 K gradually and equilibration to 300 K with a time step of 0.002 ps for 2 ns, while the time step of production was 0.002 ps for a total time of 10 ns. Parameters on saving result frequencies

**Table 2.** Interatomic Distance Constraints ( $\pm 5\%$  toleration) of Aliskiren Obtained from ROE Connectivities and Used in MD Simulations Corresponding to  $D_2O$  and DMF Solutions

hydrogen atoms	constraints (Å)	
	$D_2O$	DMF
H6–H12b	—	2.84–3.14
H4–H13	—	2.69–2.97
H12b–H15	—	2.59–2.87
H6–H13	—	2.57–2.85
H18–H20b	—	2.37–2.61
H12a–H18	—	2.50–2.78
H20b–H24	—	2.37–2.65
H3–H11	2.81–3.11	2.89–3.19
H21–H24	2.79–3.09	2.83–3.13
H9–H10	3.33–3.69	—
H16–H17b	3.07–3.39	—
H7–H11	3.30–3.64	—
H15–H17b	2.98–3.30	—
H12a–H15	2.91–3.21	—
H17b–H19	2.13–2.35	—
H19–H21	3.18–3.40	—
H12b–H23	3.17–3.39	—
H17b–H24	2.30–3.20	—
H20a–H24	2.57–2.83	—

were set in such a way in order to extract 500 conformations for each molecule. The same implicit solvent model was used as for the generation of the initial conformations, with the dielectric constant ( $\epsilon$ ) set to  $\epsilon = 81$  for the  $D_2O$  dissolved simulating conformation and  $\epsilon = 37$  for the DMF- $d_7$  dissolved simulating conformation. All minimizations had the limit of an rmsd of 0.01 Å as an energy convergence criterion.

An excessive analysis on the properties of all trajectories was made, attending thoroughly the distance properties as well as rmsd and energy values. The restrained dynamics runs for  $H_2O$  and DMF environments were analyzed for interproton distance consistency measuring the average error of distances obtained from the simulations and the NMR experimental data. The conformers' energy values were carefully examined for making a combined selection of 30 structures, corresponding to lowest energies and minimum error on restrained distances.

## ■ RESULTS AND DISCUSSION

**1. Structure Assignment.** The results of the resonance assignment of aliskiren are listed in Table 1. The  $^1H$  NMR spectrum of aliskiren in general extracted clear signals for all protons present in the molecule, except from the TFE solutions. No strong evidence implied the presence of interchanging conformers, but different conformational characteristics seem to appear between each solution environment. The complete assignment of aliskiren was accomplished using  $^1H$  NMR,  $^{13}C$  NMR, 2D ROESY, 2D HSQC, and 2D HMBC spectra.

The differences in chemical shifts between solvents are limited (Table 1). The assignment procedure led to multiple observations:

- (1)  $^1H$  TFE- $d_3$ /D<sub>2</sub>O and  $^1H$  TFE- $d_3$  spectra were identical, apart from the very specific 0.30–0.32 ppm shift to higher field on all peak values of the  $^1H$  TFE- $d_3$  spectra .

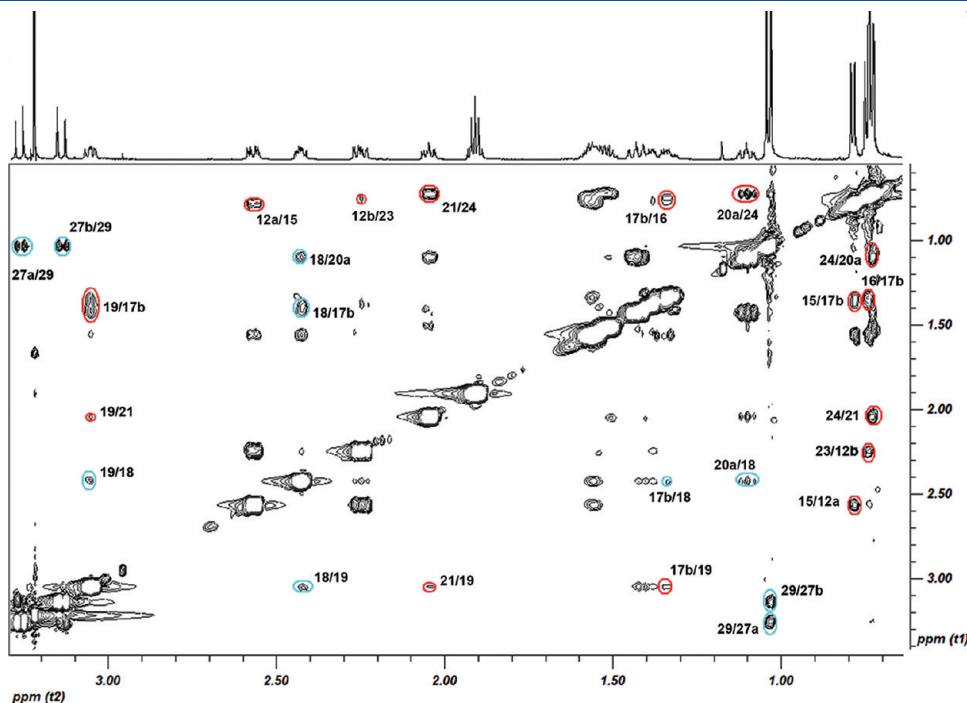


**Figure 5.** 2D ROESY spectrum of aliskiren in the region of 0.5–3.5 ppm obtained in  $D_2O$  at 25 °C. The integration limits are symbolized with curved lines. The peaks that were correspondent to non-neighboring proton–proton correlations are marked in red and were used for the MD simulations. The peaks in green were not implemented in the simulations.

Signals in  $^1\text{H}$  TFE- $d_3$ /D<sub>2</sub>O were also shifted at an average of 0.41 ppm to a lower field compared to the D<sub>2</sub>O spectrum.

- (2) The aliphatic regions appear with differences regarding the peaks corresponding to the ring, especially H6, which is strongly deshielded in the DMF- $d_7$  solvent (Figure 2a).
- (3) Protons H29 and H30 correspond to more distinct peaks in DMF- $d_7$  and TFE- $d_3$  than they do in D<sub>2</sub>O, contrary to the methyl protons H15, H16, H23, and H24, which show a more distinguishable spread in the  $^1\text{H}$  D<sub>2</sub>O spectrum.
- (4) H13, H14, H17, and H20 are collapsed in a narrow spectral area of 0.3 ppm in D<sub>2</sub>O. On the contrary, DMF- $d_7$  and TFE- $d_3$  solutions show more broadened peaks for the same protons in a wider spectral area of 0.5 ppm (Figure 2b).

**2. Structure Determination in Aqueous Solution.** 2.1.  $^1\text{H}$  NMR Resonance Assignment. The  $^1\text{H}$  NMR spectrum recorded at 10 mM aliskiren concentration (D<sub>2</sub>O, 300 K) shows fairly good resolved signals, a low degree of aggregation phenomena besides the spectral width of 1.3–1.6 ppm, and a required relatively short instrumental time for 2D-NMR data acquisition. The  $^1\text{H}$  NMR spectrum of aliskiren show one signal for each proton present in the molecule; therefore, no evidence can be found about the presence of interchanging conformers on the NMR time scale.

The  $^1\text{H}$  and  $^{13}\text{C}$  spectral assignments in water were made on the basis of the  $J$  coupling connectivities in the 2D COSY and 2D  $^1\text{H}$ – $^{13}\text{C}$  HSQC spectra (Figures 3 and 4). A logical starting point was from the H3, H4, and H6 protons of the benzyl group at 6.86, 6.74, and 6.78 ppm, respectively. Continuing with the cleanest peaks of the most deshielded H7, H11, H9, and H10 protons at 3.98, 3.69, 3.49, and 3.22 ppm, respectively, the methyl group protons of C15, C16, C23, C24, C29, and C30 were assigned in a more straightforward manner on the basis of their chemical environments and peak integration as singlets. The multiplets at the range of 1.33–1.46 and 1.49–1.60 were identified by peak integration and connectivities in the 2D  $^1\text{H}$ – $^{13}\text{C}$  HSQC spectrum. Chemical shifts were further confirmed by comparing the 2D COSY and HSQC spectra.

**2.2. Structure Calculations.** The ROESY NMR spectrum revealed important correlations between protons. These correlations were all supported by calculated interatomic distances of less than 3.50 Å and were implemented in the molecular dynamics simulations (Table 2). In particular, 27 ROEs were observed for several interatomic distances in order to be implemented in the computer calculations. Because of the large number of  $^1\text{H}$ – $^1\text{H}$  correlations (Figure 5), they were all examined thoroughly, and only distances on protons critical for the conformation of the molecule were used as distance restraints for the simulations. This led to a total of 12 constraints (Table 1), three of which (H7–H11, H12b–H23, H17a–H24) give a first indication of a “curved” conformation in the water environment.

Molecular dynamics of 20 ns total, using the restraints foreseen, generated 500 conformations, which were independently minimized. The energies among the 500 conformations were in the range from –45.91 to –28.24 kcal/mol (mean –39.14 kcal/mol), and the average distance difference per constraint used was in the range from 0.46 to 0.92 Å. The pairwise heavy atom rmsd calculated over the superposition of all the conformers had a value of  $2.30 \pm 0.68$  Å, which states a fairly good global definition

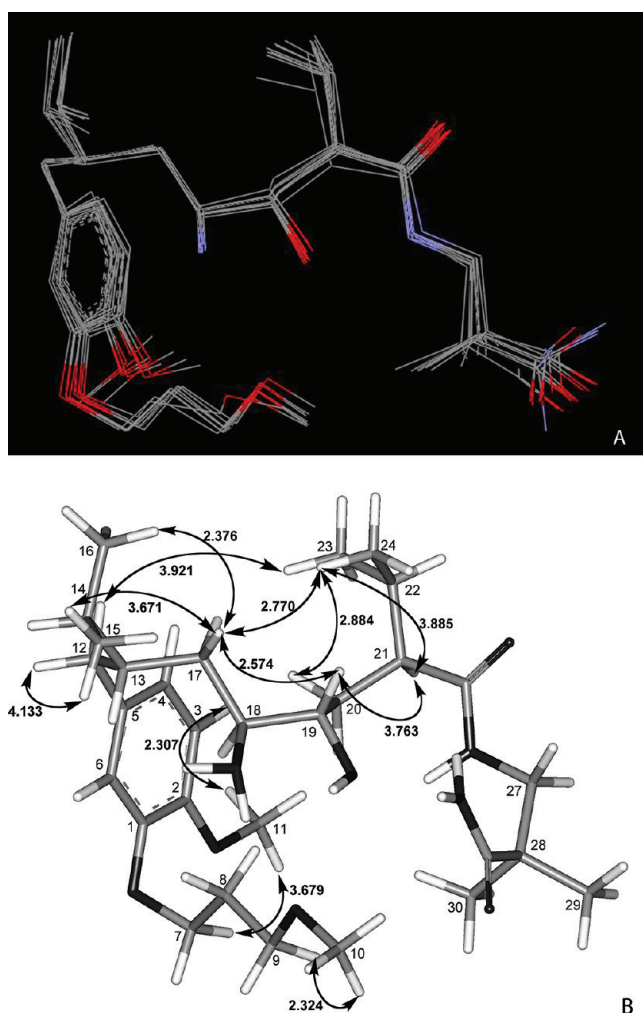


**Figure 6.** (a) The 10 lowest energy structures generated after applying restrained molecular dynamics to aliskiren in the H<sub>2</sub>O environment followed by unrestrained energy minimization (hydrogens are not shown). (b) Most representative conformation showing the selected ROESY correlations and corresponding interatomic distances (Å) of aliskiren. The key intermolecular distances between H7–H11, H12b–H23, and H17a–H24 contribute the most to this U-shaped conformation as they appear to keep these distant protons to spatial proximity.

of the conformation of the molecule. Out of this sum of optimized conformers, an ensemble of 30 conformers considered to be the most representative were selected on the basis of the following criteria: low potential energies and less divergence of interatomic distances between the constrained protons and the used constraints with values below 0.50 Å.

On the other hand, the unrestrained molecular dynamics in the water dielectric environment presented similar results but were not so straightforward in terms of a dominant conformation. These expected results showed potential energies slightly lower than the restrained dynamics, in the range from –54.42 to –28.30 kcal/mol with a difference of ~3.5 kcal/mol (mean –42.86 kcal/mol) out of the final 500 minimized structures. The notable differences were the divergence of the average distance difference per constraint extracted from the ROEs as well as the calculated heavy atom rmsd. Contrary to the restrained dynamics, the average distance difference was in range from

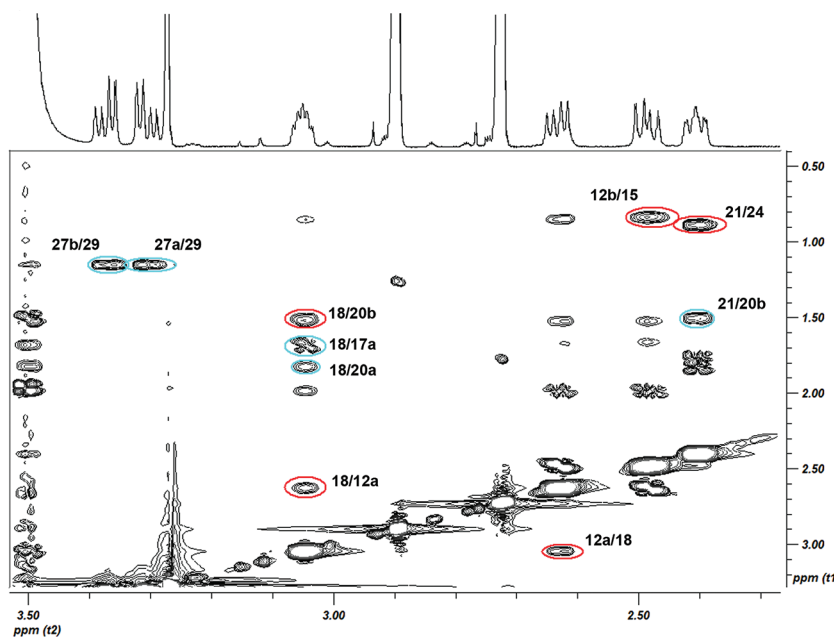


**Figure 7.** 2D ROESY spectrum of aliskiren (region vertical, 0.5–3.0 ppm; horizontal, 2.3–3.5 ppm) obtained in DMF-*d*<sub>7</sub> at 25 °C. The actual integration limits are symbolized with curved lines. The peaks in green were not implemented in the simulations. Contrary, peaks marked in red, which are correspondent to non-neighboring proton–proton correlations were used for the MD simulations. The correlation of H18 and H12 can be seen, as well as connectivities of H21 and H24, and H12 and H15 protons.

1.11 to 2.07 Å (mean 1.60 Å), and the rmsd values were much higher ( $3.59 \pm 0.99$  Å) indicating more than one dominant conformations. Despite the small differentiations in the energies between the two trajectories, the rmsd and distance variations clearly suggest that the 2D-NMR data used are of great value in determining the overall structure of aliskiren in aqueous solution, which seems to adapt a U-shape conformation (Figure 6).

**3. Structure Determination in Dimethylformamide, Trifluoroethanol and Trifluoroethanol/Water (1/1).** *3.1. <sup>1</sup>H NMR Resonance Assignment.* <sup>1</sup>H NMR spectra were recorded at a 35 mM aliskiren concentration in DMF-*d*<sub>7</sub>, TFE-*d*<sub>3</sub>, and TFE-*d*<sub>3</sub>/D<sub>2</sub>O (1:1) solvents at 300 K. The assignment of these spectra was accomplished on the basis of information gained from the D<sub>2</sub>O spectrum, which was resolved according to <sup>1</sup>H NMR, <sup>13</sup>C NMR, 2D ROESY, and 2D HSQC experiments.

DMF-*d*<sub>7</sub> as a solvent resulted in better resolution in all peaks, showing one signal for each proton present in the molecule (SF4). Protons of C12, C17, C20, and C27 had all different peaks, each of which were renamed as H12a, H12b, C17a, C17b, H20a, H20b, H27a, and H27b (Figure 1) and were further ascertained with the coupling constants of theforesaid peaks. Different variations of the chemical shift  $\Delta\nu$  values were reported compared to the aqueous solution having a lower average of 0.18 ppm. Again, as in the D<sub>2</sub>O spectrum, no evidence of multiple conformers was found. A broadening effect is observed in the 1.2–1.8 region, where in the DMF-*d*<sub>7</sub> spectrum along with a good resolution in the chemical shifts, assisted in the assignment of these peaks in combination with the connectivities in the 2D <sup>1</sup>H–<sup>13</sup>C HSQC spectrum. Likewise, the H15, H16, H23, and H24 proton corresponding peaks were identified with ease, showing a fairly good broadening through the spectrum. 2D ROESY experiments were acquired in order to further examine the conformational properties of aliskiren in the dimethylformamide solution.

The <sup>1</sup>H NMR spectrum of trifluoroethanol and trifluoroethanol/water (50%) showed similarities to the ones predetermined. Although there was a reasonable resolution through the proton signals and splitting of the same peaks as in the previous solvents, a high percentage of shouldering of the methyl groups' hydrogens was observed. Another obstacle was many broadening effects though the signals (SF5), therefore, not ensuring a high sensitivity of the NOESY experiments. The <sup>1</sup>H TFE-*d*<sub>3</sub>/D<sub>2</sub>O and <sup>1</sup>H TFE-*d*<sub>3</sub> spectra were identical apart from the very specific 0.30–0.32 ppm shift on all peak values.

**3.2. Structure Calculations.** According to the ROESY experiment on the DMF-*d*<sub>7</sub> solution, 23 <sup>1</sup>H–<sup>1</sup>H correlations were found. The calculated interatomic distances were examined thoroughly, and only correlations on protons of non-neighboring carbons were used for further molecular dynamics simulations. Figure 7 depicts a region with some “non-expected” <sup>1</sup>H–<sup>1</sup>H connectivities between H12a and H18 as well as H21 and H24, which later revealed some *cis*-bonding in some dihedrals of the molecule. Apart from these connections, the selected ROEs of theoretically distant protons showed the following correlations: H12 with both H6 and H15, H13 with both H4 and H6, H18 with both H12 and H20, and H24 with H20 as well as H3 with H11. The 12 selected distances of less than 3.20 Å, whereas most were approximately 2.70 Å, were used as constraints for the simulations regarding DMF as a solvent for aliskiren.

Again, as with the H<sub>2</sub>O ROEs procedure, a molecular dynamics simulation of 20 ns total was performed, using the restraints which generated 500 conformations that were independently minimized. The energies calculated among the 500 conformations (SF6) were in the range from –45.63 to –28.38 kcal/mol with a mean value of –35.77 kcal/mol. The average distance difference per constraint used ranged from 0.29 to 0.64 Å. The pairwise heavy atom rmsd was calculated over the superposition of all the

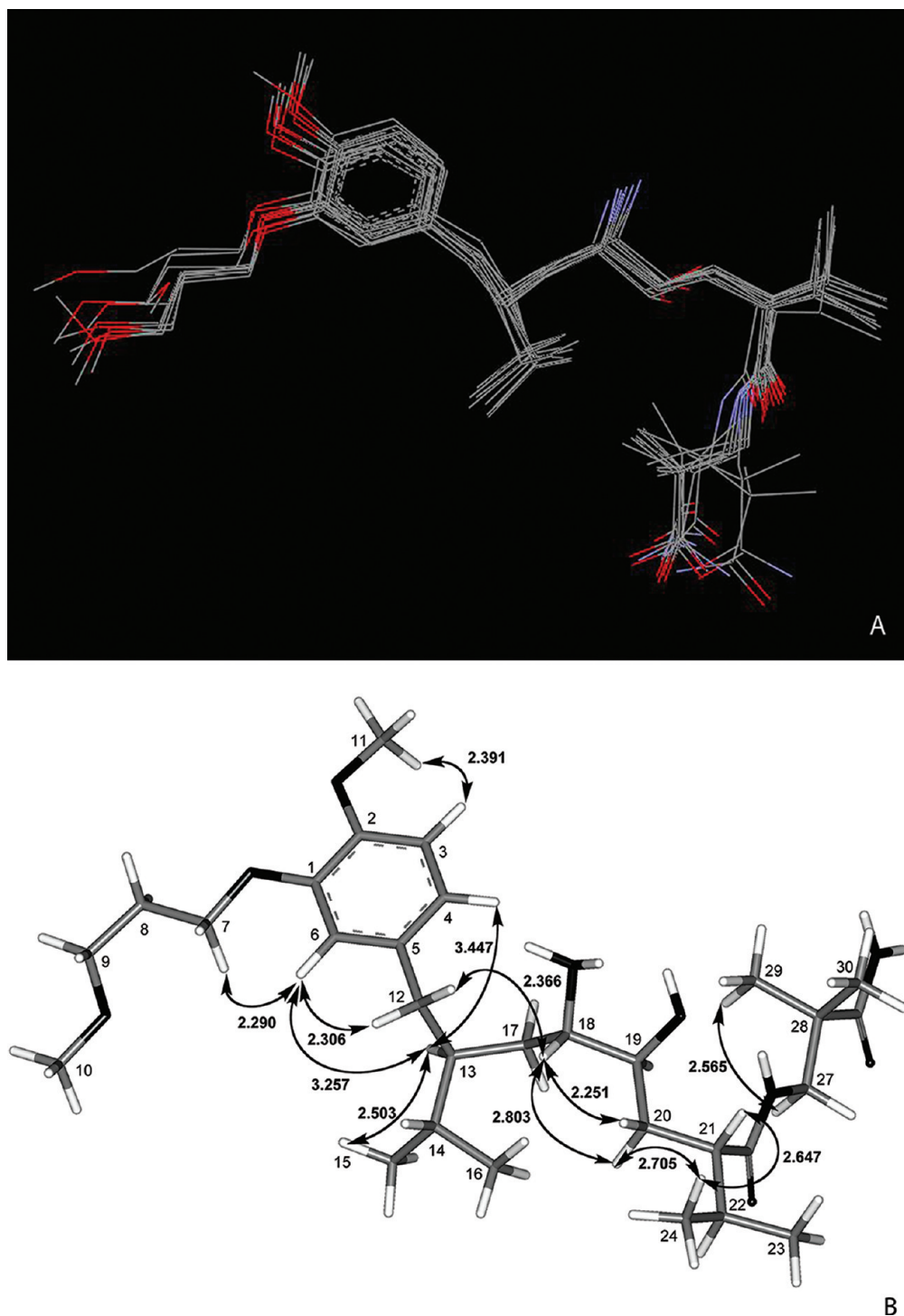


**Figure 8.** (a) Ten lowest energy structures generated after applying restrained molecular dynamics to aliskiren in the DMF environment followed by unrestrained energy minimization (hydrogens are not shown). (b) Most representative conformation showing the selected ROESY correlations and corresponding interatomic distances ( $\text{\AA}$ ) of aliskiren. Intermolecular distances between H6–H7 indicate the formation of a *cis*-bond between C6–C1–O32–C7, but no ROEs connect very distant protons, which implies an “extended” conformation of the molecule in the examined solvent.

conformers with a value of  $2.49 \pm 0.87 \text{ \AA}$ , which states a single conformation of the molecule (SF7). Out of this sum of optimized conformers, again an ensemble of 30 conformers considered to be the most representative were selected on the basis of the following criteria: low potential energies and less

divergence of interatomic distances between the constrained protons and the used constraints with values below  $0.40 \text{ \AA}$ . Out of these 30 conformations, 10 are illustrated in panel (a) of Figure 8 in a superimposed state, giving a 3D view of the molecules’ heavy atoms relative orientation when in DMF solution. The most

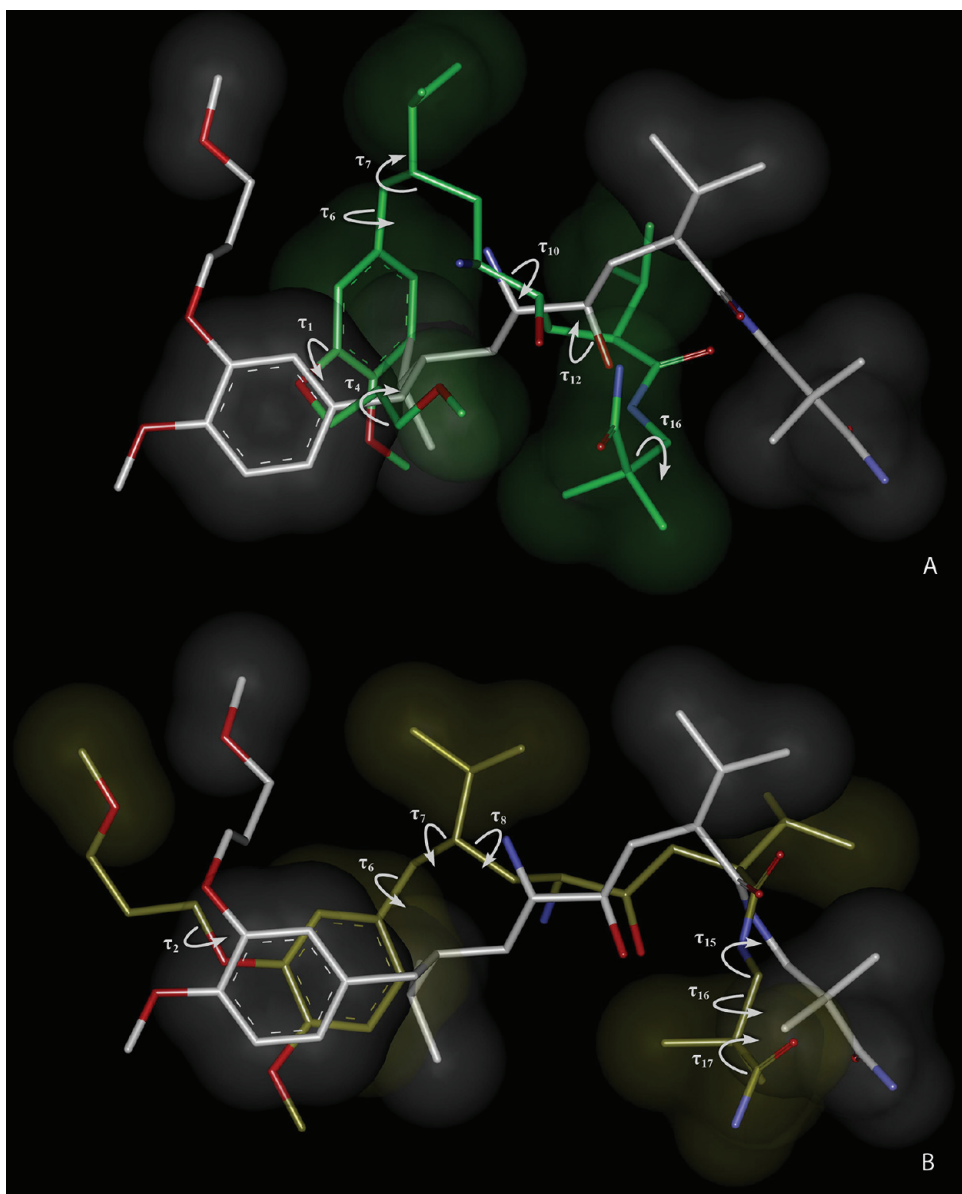


**Figure 9.** (a) Superimposition of aliskiren crystal conformation (white) with aqueous solvent structure (green) according to heavy atom rmsd fit. Hydrogens are not present for better clarity of the relative positions of heavy atoms, where dihedrals presenting high diversity most responsible for differentiation between structures are displayed in gray arrows. (b) Superimposition of aliskiren crystal conformation (white) with the DMF solvent structure (yellow) according to heavy atom rmsd fit. Hydrogens are not present for better clarity of the relative positions of heavy atoms, where dihedrals presenting high diversity most responsible for differentiation between structures are displayed in gray arrows.

representative conformation in terms of low potential energy and good convergence of the ROEs used in the simulation is shown in panel (b) of Figure 8, where the relative orientations of C3, C4, C6, C11, C12, C13, C15, C18, C20, C21, and C24 were determined.

A second molecular dynamics run of 10 ns with the dielectric constant set to  $\epsilon = 37$  and without the use of distance restraints was again performed on the molecule in order to evaluate the results of the restrained dynamics. The results were different in terms of a dominant conformation, potential energies, and rmsd values. The lower potential energies of the final S00 minimized structures were in the range from  $-54.93$  to  $-31.50$  kcal/mol (mean  $-43.73$  kcal/mol) and when compared the restrained dynamics had an average difference of  $\sim 8$  kcal/mol.

Consecutively, the average distance difference per constraint extracted from the ROEs as well as the calculated heavy atom rmsd were calculated. Contrary to the restrained dynamics, the average distance difference was in range from  $0.39$  to  $1.11$  Å (mean  $0.73$  Å), and the rmsd values were much higher ( $3.48 \pm 0.96$  Å), indicating more than one dominant conformation. In the DMF solvent models, the rmsd and distance constraint differentiations again substantiate that the 2D-NMR data used are of great value in determining the overall structure of the molecule in this specific environment.

**4. Comparison of the Proposed Conformations in Different Solutions with the One Obtained from the Renin-Aliskiren Crystal Structure.** The resolved conformations for aliskiren in aqueous and DMF solutions present quite distinct

**Table 3.** Dihedral Angle Values and Net Differences between the Crystal Bound H<sub>2</sub>O and DMF Structure<sup>a</sup>

	$\tau_1$	$\tau_2$	$\tau_3$	$\tau_4$	$\tau_5$	$\tau_6$	$\tau_7$	$\tau_8$	$\tau_9$	$\tau_{10}$	$\tau_{11}$	$\tau_{12}$	$\tau_{13}$	$\tau_{14}$	$\tau_{15}$	$\tau_{16}$	$\tau_{17}$	$\tau_{18}$	$\tau_{19}$	$\tau_{20}$
crystal structure	-164.03	74.44	175.65	-51.20	140.88	-58.48	-175.41	-97.30	177.13	-161.93	-176.01	-51.80	118.83	-176.62	-119.60	63.25	60.84	-0.51	-65.07	-55.01
H <sub>2</sub> O structure	65.22	54.94	161.58	-176.38	178.01	66.90	58.95	-93.92	169.52	-83.44	155.10	46.51	38.63	172.01	160.69	-84.35	21.66	-0.65	162.48	62.12
DMF structure	-169.27	175.90	-173.45	-59.75	-178.12	94.62	75.45	68.54	156.79	-131.89	-164.45	-55.74	86.43	174.94	178.13	176.59	172.83	16.63	67.90	-52.29
net difference crystal-H <sub>2</sub> O	130.75	19.50	14.06	125.18	37.13	125.38	<b>125.64</b>	3.38	7.60	<b>78.48</b>	28.89	<b>98.31</b>	<b>80.21</b>	11.37	41.09	<b>147.60</b>	39.18	0.14	132.45	117.13
net difference crystal-DMF	5.24	<b>101.46</b>	10.90	8.55	41.00	<b>153.11</b>	<b>109.14</b>	<b>165.84</b>	20.34	30.03	11.56	3.93	32.41	8.44	72.37	<b>113.34</b>	<b>111.99</b>	17.14	132.96	2.72
net difference H <sub>2</sub> O-DMF	125.51	129.16	24.97	116.62	3.87	27.72	16.50	162.46	12.73	48.45	40.45	102.25	47.80	2.93	17.44	98.96	151.17	17.28	94.58	114.41

<sup>a</sup> Net difference denoted as difference between the absolute values. Bold values denote over 70° divergence.

differences in their spatial characteristics and specifically in the relative orientation of the carbon C5 to C31 chains. The bound conformation of the molecule obtained from the renin–aliskiren crystal structure complex was superimposed with the two dominant conformers according to their heavy atoms in order to extract information on the dihedrals values and the orientation of the different pharmacophoric groups (Figure 9). The groups space occupying the receptor’s binding pockets S1, S3, S3<sup>SP</sup>, S1', and S2'<sup>19</sup> is highlighted for a better understanding of their orientation compared to that of the crystal bound conformation of aliskiren. Important differentiations for the H<sub>2</sub>O conformation can be seen in values of dihedrals  $\tau_1$ ,  $\tau_4$ ,  $\tau_6$ ,  $\tau_7$ ,  $\tau_{10}$ ,  $\tau_{12}$ ,  $\tau_{13}$ , and  $\tau_{16}$ , whereas a crucial role in the DMF conformation is played by dihedrals  $\tau_2$ ,  $\tau_6$ ,  $\tau_7$ ,  $\tau_8$ ,  $\tau_{15}$ ,  $\tau_{16}$ , and  $\tau_{17}$  as shown in Table 3. The difference in  $\tau_1$  and  $\tau_4$ , driven by the H7–H11 ROE constraint in the aqueous conformer, gives the C1–C10 carbon chain an orientation toward C11. Values of dihedral  $\tau_6$  vary, showing three different orientations of the large carbon chain of C5–C31, giving a distinct conformation for each H<sub>2</sub>O and DMF conformers. Torsion  $\tau_{10}$  as part of the two chiral centers, C18 and C19, is very important for the situation of the carbon chain C18–C31. Structural similarities, based on heavy atom superimposition and rmsd calculations, indicate that the DMF conformation is relatively closer to the crystal structure having an rmsd value of 6.538 Å, while the aqueous structure records a value of 8.336 Å compared to the crystal structure.

Apart from the significantly “curved” structures of this antihypertensive agent in H<sub>2</sub>O and DMF, the essential structural difference is the position of the “backbone” of the molecule, which in the case of the H<sub>2</sub>O environment (H7–H11, H12b–H23, and H17b–H24 ROEs in Table 1 indicating proximity of distant protons) is oriented parallel to the phenyl ring plane. Contrary, the structure reported for aliskiren in the DMF solvent appears to have the main chain oriented to the side rather than parallel to the ring. In general, the two different solvents impose a “curved” structure in both cases but a different orientation to the pharmacophoric groups. Nevertheless, the DMF structure’s pharmacophoric groups are definitely closer to the ones from the crystal structure, whereas the H<sub>2</sub>O conformation is “severely” curved with very little matching of these crucial spatial requirements. For this reason, an rmsd calculation based on the pharmacophoric groups only (including hydrogens) that occupy the S1, S3, S3<sup>SP</sup>, S1', and S2' subpockets of renin showed a better matching than 3.82 Å for the DMF conformation compared to a value of 5.86 Å for the aqueous conformation.

For acquiring a better understanding on a theoretical approach of the energy barriers between the two conformations in solutions and the bound to the protein conformation, a series of 1 ns molecular dynamics was performed in 300 K using a dielectric constant equal to 81. Dihedral restraints of torsions  $\tau_1$ – $\tau_{16}$  were defined for the solution conformations, with a force constant of 5 kcal/mol, and applied after a short time of equilibration of the molecule. MD results show that approximately ~29 kcal/mol was needed for the conformation of aliskiren in DMF to adapt similarly to the bound conformation, whereas approximately 40 kcal/mol was needed for the conformation in H<sub>2</sub>O to adapt to the bound conformation’s characteristics (Figure 10). The heavy atom rmsd values of the final conformations after the MD, compared to bound structure’s conformation, were calculated and were in the range from 1.21 to 1.79 Å immediately after the adaptation of the bioactive conformation. The transition of the DMF structure,

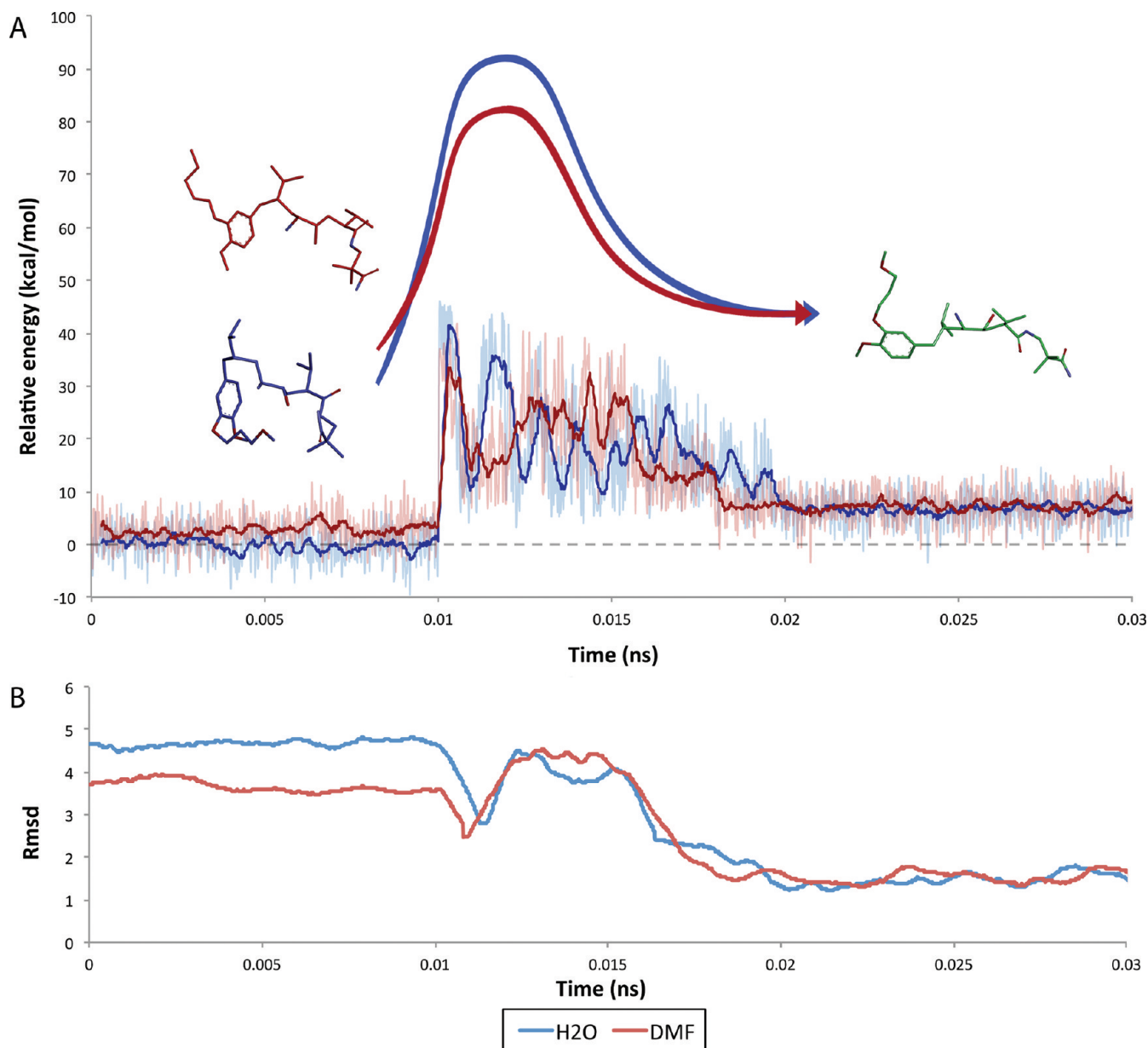


**Figure 10.** (a) Relative potential energy curves of the first 0.03 ns of the MD procedure where torsional constraints were applied for transition of the two solution structures into the bound conformation obtained from the crystal structure. Constraints were applied in time point 0.01 ns. (b) The rmsd of the conformations produced in each dynamics run to the bound structure plotted against time.

approached from a theoretical point of view as the solution environment is different than of the receptors' one, demonstrates that it has more similar features to the bound one as it requires less energy to overcome the barrier. On the other hand, this study also demonstrates the facile transition of the aqueous aliskiren conformation to the bound one, which verifies the flexibility of the molecule.

## CONCLUSION

In this work, we present NMR data, 1D and 2D, regarding aliskiren in various solvents combined with molecular modeling techniques in order to clarify their structural characteristics. 2D-NMR constraints were performed for extracting connectivities between protons for the molecule in H<sub>2</sub>O and DMF solutions and implemented in molecular dynamics simulations. Aliskiren as a lipophilic molecule tends to have a more extended

conformation in DMF, which is a less polar solvent than H<sub>2</sub>O. The final structure of aliskiren in the aqueous environment is less similar to the one extracted from the renin–aliskiren crystallized complex, having a more “curved” arrangement between heavy atoms, which is a result of strong interproton interactions of seemingly distant hydrogens. The DMF heavy atom orientation is less “curved” where interproton interactions between distant hydrogens are not shown by the 2D-NMR data, indicating that in general the two different solvents impose a different orientation to the pharmacophoric groups of the molecule.

## ASSOCIATED CONTENT

**S Supporting Information.** Figure S1 with spectrum of the 2D COSY experiments in D<sub>2</sub>O solvent. Figures S2 and S3 giving

results of heteronuclear HSQC and HMBC spectra. Figures S4 and S5 show  $^1\text{H}$  NMR spectra of aliskiren obtained at 25 °C in DMF- $d_7$  and TFE- $d_3$  solvents respectively. Figure S6 reports the potential energies reported for each molecular dynamics trajectory, whereas Figure S7 shows the heavy atom rmsd values for the lowest energy conformation of each molecular dynamics trajectory. Figure S8 illustrates a superposition of the two final structures with the aliskiren crystal conformation according to the ring carbons for a better clarity of the results. This material is free of charge via the Internet at <http://pubs.acs.org>.

## AUTHOR INFORMATION

### Corresponding Author

\*Tel: +30 2610 997905. Fax: +30 2610 997180. E-mail: tselios@upatras.gr.

## ACKNOWLEDGMENT

We gratefully acknowledge the support of ELDRUG SA, Patras Science Park, Greece. We thank Prof. Leonardo Pardo (Universitat Autònoma de Barcelona) for computer facilities and software use, as well as Ivan R. Rodriguez for expert help on experimental procedures.

## REFERENCES

- (1) de Gasparo, M.; Catt, K. J.; Inagami, T.; Wright, J. W.; Unger, T. International union of pharmacology. XXIII. The angiotensin II receptors. *Pharmacol. Rev.* **2000**, *52*, 415–472.
- (2) Mantzourani, E.; Laimou, D.; Matsoukas, M. T.; Tselios, T. Peptides as therapeutic agents or drug leads for autoimmune, hormone dependent and cardiovascular diseases. *Anti-Inflammatory Anti-Allergy Agents Med. Chem.* **2008**, *7*, 294–306.
- (3) Hunyady, L.; Catt, K. J. Pleiotropic AT1 receptor signaling pathways mediating physiological and pathogenic actions of angiotensin II. *Mol. Endocrinol.* **2006**, *20*, 953–970.
- (4) Skeggs, L. T.; Dorer, F. E.; Levine, M.; Lentz, K. E.; Kahn, J. R. The biochemistry of the renin–angiotensin system. *Adv. Exp. Med. Biol.* **1980**, *130*, 1–27.
- (5) Greenlee, W. J. Renin inhibitors. *Med. Res. Rev.* **1990**, *10*, 173–236.
- (6) Wood, J. M.; Cumin, F.; Maibaum, J. Pharmacology of renin inhibitors and their application to the treatment of hypertension. *Pharmacol. Ther.* **1994**, *61*, 325–344.
- (7) Lefevre, G.; Duval, M.; Poncin, A. Direct micro-radioimmunoassay of the new renin inhibitor CGP 60536. *J. Immunoassay* **2000**, *21*, 65–84.
- (8) Paulis, L.; Unger, T. Novel therapeutic targets for hypertension. *Nat. Rev. Cardiol.* **2010**, *7*, 431–441.
- (9) Staessen, J. A.; Li, Y.; Richart, T. Oral renin inhibitors. *Lancet* **2006**, *21*, 1449–1456.
- (10) Weir, M. R. Renin inhibitors: Novel agents for renoprotection or a better angiotensin receptor blocker for blood pressure lowering? *Curr. Opin. Nephrol. Hypertens.* **2007**, *16*, 416–421.
- (11) Azizi, M. Direct renin inhibition: Clinical pharmacology. *J. Mol. Med.* **2008**, *86*, 647–654.
- (12) Fisher, N. D. L.; Hollenberg, N. K. Renin inhibition: What are the therapeutic opportunities? *J. Am. Soc. Nephrol.* **2005**, *16*, 592–599.
- (13) Goschke, R.; Stutz, S.; Rasetti, V.; Cohen, N. C.; Rahuel, J.; Rigollier, P.; Baum, H. P.; Forgiarini, P.; Schnell, C. R.; Wagner, T.; Gruetter, M. G.; Fuhrer, W.; Schilling, W.; Cumin, F.; Wood, J. M.; Maibaum, J. Novel 2,7-dialkyl-substituted 5(S)-amino-4(S)-hydroxy-8-phenyl-octanecarboxamide transition state peptidomimetics are potent and orally active inhibitors of human renin. *J. Med. Chem.* **2007**, *50*, 4818–4831.
- (14) Maibaum, J.; Feldman, D. L. Renin inhibitors as novel treatments for cardiovascular disease. *Expert Opin. Ther. Pat.* **2003**, *13*, 583–603.
- (15) Gradman, A. H.; Pinto, R.; Kad, R. Current concepts: Renin inhibition in the treatment of hypertension. *Curr. Opin. Pharmacol.* **2008**, *8*, 120–126.
- (16) Hollenberg, N. K. Renin inhibition. *Hypertension* **2008**, *25*, 70–76.
- (17) Maibaum, J.; Stutz, S.; Goschke, R.; Rigollier, P.; Yamaguchi, Y.; Cumin, F.; Rahuel, J.; Baum, H. P.; Cohen, N. C.; Schnell, C. R.; Fuhrer, W.; Gruetter, M. G.; Schilling, W.; Wood, J. M. Structural modification of the P2' position of 2,7-dialkyl-substituted 5(S)-amino-4(S)-hydroxy-8-phenyl-octanecarboxamides: the discovery of aliskiren, a potent non-peptide human renin inhibitor active after once daily dosing in marmosets. *J. Med. Chem.* **2007**, *50*, 4832–4844.
- (18) Vaidyanathan, S.; Valencia, J.; Kemp, C.; Zhao, C.; Yeh, C. -M.; Bizot, M. N.; Denouel, J.; Dieterich, H. A.; Dole, W. P. Lack of pharmacokinetic interactions of aliskiren, a novel direct renin inhibitor for the treatment of hypertension, with the antihypertensives amlodipine, valsartan, hydrochlorothiazide (HCTZ) and ramipril in healthy volunteers. *Int. J. Clin. Pract.* **2006**, *60*, 1343–1356.
- (19) Laimou, D. K.; Katsara, M.; Matsoukas, M. -T.; Apostolopoulos, V.; Troganis, A. N.; Tselios, T. V. Structural elucidation of Leuprolide and its analogues in solution: Insight into their bioactive conformation. *Amino Acids* **2010**, *39*, 1147–1160.
- (20) Mantzourani, E. D.; Tselios, T. V.; Grdadolnik, S. G.; Platts, J. A.; Brancale, A.; Deraos, G. N.; Matsoukas, J. M.; Mavromoustakos, T. M. Comparison of proposed putative active conformations of myelin basic protein epitope 87–99 linear altered peptide ligands by spectroscopic and modelling studies: The role of positions 91 and 96 in T-cell receptor activation. *J. Med. Chem.* **2006**, *49*, 6683–6691.
- (21) Mantzourani, E. D.; Platts, J. A.; Brancale, A.; Mavromoustakos, T. M.; Tselios, T. V. Molecular dynamics at the receptor level of immunodominant myelin basic protein epitope 87–99 implicated in multiple sclerosis and its antagonists altered peptide ligands: triggering of immune response. *J. Mol. Graph. Model.* **2007**, *26*, 471–481.
- (22) Spyrianti, Z.; Dalkas, G. A.; Spyroulias, G. A.; Mantzourani, E. D.; Mavromoustakos, T.; Friligou, I.; Matsoukas, J. M.; Tselios, T. V. Putative bioactive conformations of amide linked cyclic myelin basic protein peptide analogues associated with experimental autoimmune encephalomyelitis. *J. Med. Chem.* **2007**, *50*, 6039–6047.
- (23) Wood, J. M.; Maibaum, J.; Rahuel, J.; Grutter, M. G.; Cohen, N. -C.; Rasetti, V.; Ruger, H.; Stutz, S.; Fuhrer, W.; Schilling, W.; Rigollier, P.; Yamaguchi, Y.; Cumin, F.; Baum, H.-P.; Schnell, C. R.; Herold, P.; Mah, R.; Jensen, C.; O'Brien, E.; Stanton, A.; Bedigan, M. P. Structure-based design of aliskiren, a novel orally effective renin inhibitor. *Biochem. Biophys. Res. Commun.* **2003**, *308*, 698–705.
- (24) Waldmeier, F.; Glaenzel, U.; Wirz, B.; Oberer, L.; Schmid, D.; Seiberling, M.; Valencia, J.; Riviere, G. –J.; End, P.; Vaidyanathan, S. Absorption, distribution, metabolism, and elimination of the direct renin inhibitor aliskiren in healthy volunteers. *Drug Metab. Dispos.* **2007**, *35*, 1418–1428.
- (25) Rahuel, J.; Rasetti, V.; Maibaum, J.; Rueger, H.; Goschke, R.; Cohen, N. C.; Stutz, S.; Cumin, F.; Fuhrer, W.; Wood, J. M.; Grutter, M. G. Structure-based drug design: The discovery of novel nonpeptide orally active inhibitors of human renin. *Chem. Biol.* **2000**, *7*, 493–504.
- (26) Griesinger, C.; Ernst, R. R. Frequency offset effects and their elimination in NMR rotating-frame cross-relaxation spectroscopy. *J. Magn. Reson.* **1987**, *75*, 261–271.
- (27) Ryckaert, J. –P.; Ciccotti, G.; Berendsen, H. J. C. Numerical integration of the cartesian equations of motion of a system with constraints: Molecular dynamics of *n*-alkanes. *J. Comp. Phys.* **1977**, *23*, 327–341.

## NOTE ADDED AFTER ASAP PUBLICATION

This paper was published ASAP on August 10, 2011, with minor text errors. The corrected version was published ASAP on August 29, 2011.